Nuclear Instruments and Methods in Physics Research B 123 (1997) 271–274

ELSEVIER

NIM B
Beam Interactions with Materials & Atoms

High resolution AMS imaging of radiocarbon in biomedical applications

Z.X. Jiang [a,c], C. Bronk Ramsey [a], R.E.M. Hedges [a,*], P. Somogyi [b], J.D.B. Roberts [b], A. Cowey [c]

[a] *Radiocarbon Accelerator Unit, Oxford University, 6 Keble Road, Oxford, OX1 3QJ, UK*
[b] *MRC Anatomical Neuropharmacology Unit, Oxford University, Mansfield Road, Oxford, OX1 3QT, UK*
[c] *Department of Experimental Psychology, Oxford University, South Parks Road, Oxford, OX1 3UD, UK*

Abstract

Radiocarbon has been an important labelling element in biological metabolism studies. By interfacing an accelerator mass spectrometer (AMS) with a scanning microprobe secondary ion source, we have imaged the uptake of radiocarbon labelled metabolic or neurotransmitter amino acids by neurons and glial cells of rats and gerbils at high resolution (1 micron), high sensitivity and in a short time. The biological samples are prepared and sectioned serially at 0.5 μm thickness using standard histological procedures. The adjacent sections to those used for AMS imaging were either immunolabelled with antibodies to GABA to reveal GABA-containing cells, or stained with toluidine blue to visualise every cell. Therefore, the distribution of radiocarbon revealed by AMS could be matched to that of the cells. By simultaneously measuring the ^{14}C, ^{13}C and ^{12}C signals, we can demonstrate that the localised peaks of radiocarbon could be readily identified and matched to GABA-immunopositive neurons and glial cells by aligning the radiocarbon deficient blood vessels with the vessels in the adjacent histologically stained section. The results revealed the selective uptake of the neurotransmitter, GABA and that of metabolic amino acid, leucine. The technique compares favourably with high resolution autoradiography and provides great potential for improving the analysis of molecular interactions in and between cells.

1. Introduction

Radiocarbon has been widely used in biological studies as an important labelling element. Until recently, however, its application has been limited by the long exposure time and low spatial resolutions in autoradiography. With the development of ion microprobe of increased beam intensity and reduced spot size into the sub-micron domain, secondary ion mass spectroscopy imaging has been increasingly used to study metabolic activities of important trace elements/isotopes such as C, N, Ca, K, Mg, Al, Cl and I [1].

Accelerator mass spectrometer (AMS) is the fast and sensitive method for radiocarbon detection. The AMS at Oxford is normally dedicated to radiocarbon measurements and detects secondary C^- ions as single $^{14}C^{3+}$ ions with an overall efficiency of about 25% ~ 30% [2]. By interfacing an AMS with a secondary ion source based on a scanning liquid metal ion microprobe sputtering biological samples, we have developed a high resolution, high sensitivity and fast radiocarbon imaging instrument [3–5]. We can map the distribution of C^{14}-labelled molecules, such as amino acids, in the brain of animals (e.g. rats or gerbils) allowing a period of metabolism, so that the selective uptake and transport of the amino acids by certain neurons and other cells can be revealed [6,7].

2. Imaging AMS

A liquid metal Ga^+ microprobe of 1nA beam current and 10 keV ion energy with spot size of 1 micron diameter (at present) is rastered across the sample to generate negative atomic and molecular ions. These secondary ions are injected into a tandem electrostatic accelerator with the sample stage biased at -14 kV. This bias is essential for the injection of the secondary ions and consequently the probe ion energy is 24 keV. As this bias voltage is comparable to the probe ion accelerating voltage, it inevitably compromises the beam quality and affects the scanning area. The scanning area and beam spot size is monitored in real-time by dropping a metal target into the beamline before the entrance to the accelerator and using a PMT/Scintillator to detect the secondary electrons generated by these secondary ions. The image of a copper mesh

* Corresponding author. Fax: +44-1865-273932; email: orau@rlaha.ox.ac.uk.

0168-583X/97/$17.00
PII S0168-583X(96)00630-1

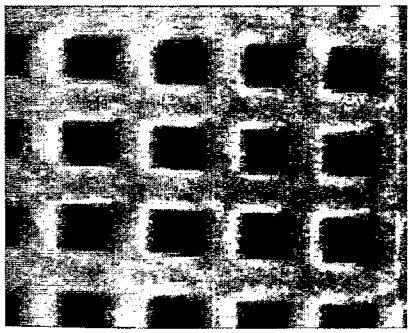

Fig. 1. Directly injected secondary ion image of a copper mesh (Cu 2000) with grid width of 6 μm.

(Cu 2000 mesh) with grid width of 6 μm is shown in Fig. 1. This arrangement overcomes the problems of noise found with a secondary electron within the source. Those are caused by the caesiation of the sample which is in one hand essential for the high yield of negative ions but, on the other hand, causes spontaneous electron emission from the aluminium sample stage at a bias of −14 kV.

The secondary negative ions generated from histologically prepared samples of brain tissue are mainly O^- C^-, C_2^- CH^- and CN^-. This is in accordance with their electron affinities and the natural abundance in the composition of the biological materials [3,4]. As the high yield of the secondary ions, in particular C^- is essential for the high resolution and fast imaging of radiocarbon, the sample surface needs to be treated with caesium. This is achieved by heating a custom-made Cs spray whose nozzle is close to the sample surface. Consequently, C^- yield has been increased by a factor of 25 ~ 30 to 5% of the primary Ga^+ flux and makes C^- the strongest secondary ion peak. The radiocarbon detection is achieved by injecting C^- at initial energy of 14 keV into a tandem accelerator with a gas stripper which generates C^{3+} at an energy of 8 MeV with a transmission efficiency of ~25% to 30%. The AMS can also be used for other atomic and molecular ions such as [$CN^- \rightarrow C^{3+}$ or $^{15}N^{3+}$], though these are not the main subject of this paper.

The sputtering rate for the biosample, which is tissue embedded in epoxy resin, is measured to be ~10 $\mu m/Acm^{-2}s$, thus the sputtering ion yield of C^-/C is calculated to be 0.01. Therefore, the detection efficiency of the AMS system as a whole is 0.25% in relation to the carbon content of the sample. In other words, for the detection of every ^{14}C, 400 of them need to be sputtered. Radiocarbon imaging has been achieved by collecting the $^{14}C^{3+}$ counts for each scanning microprobe pixel. The minimal size of the pixel is the spot size, currently 1 μm in diameter. To build an image of a biosample of a certain thickness, say 0.5 μm (serially sectioned), the required minimum radiocarbon labelling concentration is inversely proportional to the square of the beam spot diameter. That is, the smaller the spot diameter, the smaller the volume to be sputtered, hence the higher ^{14}C concentration for the required count of the $^{14}C^{3+}$. As it takes 0.3 seconds to sputter through the 0.5 μm thick sample, or *pixel volume* of 0.4 μm^3 and assuming the carbon atom density of $2.5 \times 10^{10}/\mu m^3$, a total number of 1×10^{10} carbon atoms are sputtered per pixel. For at least 1 ^{14}C count per pixel, this limits the minimum required radiocarbon labelling concentration of C^{14}/C^{12} to be 4×10^{-8}. This is 40000 times higher than the natural background ($^{14}C/^{12}C = 10^{-12}$). As a result of using the AMS system, the background is found to be negligible by using unlabelled biosamples [4]. It is clear that the necessary radiocarbon labelling concentration (mC) in the biosample for AMS imaging is related to the beam spot size d (the image resolution), the sample carbon atom density (ρ), the sputtering rate (spr), the ion beam intensity (i), the dwell time (τ), the sputtering yield (γ), and the AMS detection efficiency (ϵ), as formulated in the following equation:

$$mC = \frac{^{14}C}{^{12}C} = \frac{1/\text{pixel}}{\epsilon \times \gamma \times 1/4 \times \pi \times d^2 \times \tau \times spr \times i \times \rho} \quad (1)$$

assuming an average of one ^{14}C count per pixel is required.

In the experiment, the $^{14}C^{3+}$ ion is kinematically filtered and detected by gas proportional counting, while more abundant ions such as $^{13}C^{3+}$ or $^{12}C^{3+}$ are detected respectively by a silicon surface barrier detector and a small aperture PMT/Scintillator or alternatively a Faraday cup. Thus the stable carbon isotopes can be mapped simultaneously, so that the ^{14}C can be located and quantified in relation to the normal carbon feature of the biosamples. This also allows a quantitative C^{14}/C^{12} measurement and compensation for yield variations, for example due to edge effects. As the typical $^{12}C^{3+}$ current for the Cs treated biosamples is in the range of 10 ~ 50 pA, the silicon surface barrier detector has a very limited life time even used for $^{13}C^{3+}$ only. We have designed and installed a small aperture PMT/Scintillator with a drop-in target. The target of copper is enclosed in a grounded stainless steel enclosure with a small beam entry aperture of ~6 mm. The copper target is biased at −10 kV to accelerate the secondary electrons generated by the 8 MeV ions to the scintillator to be detected as photon signals. The bias also prevented other electrons from entering the enclosure. We have measured that the yield of the secondary electron for 8 MeV $^{12}C^{3+}$ is ~10. The detection efficiency is 3.5% at the time of writing.

3. Biomedical applications

We have studied the selective uptake of a C^{14}-labelled neurotransmitter, C^{14}-GABA (4-amino-n-[U-C^{14}] butyric

acid), by neurons having GABA carriers and using GABA as transmitter, and also by glial cells. Radiolabelled GABA was microinjected in vivo into the occipital visual cortex of the rat brain. Along each injection track (4–5 mm tangentially, latero-ventral from the pia and 5–8 injection in 0.5 mm steps), a total of 0.75 μl GABA (0.15 μCi, or 5550 Bq) has been delivered over a period of 15 min. The C^{14}-GABA is taken up by those neurons that have high affinity uptake proteins for GABA and have axons and terminals at the injection site. After allowing for the transport of GABA (~ 50 min), the brain tissue was perfused through the vasculature with a mixture of paraformaldehyde and glutaraldehyde, in order to bind covalently the accumulated transmitter to proteins. The tissue was embedded in epoxy resin and sectioned serially at 0.5 μm using standard histological procedures as required for electron microscopic material. The two adjacent sections to those used for AMS imaging were either stained with toluidine blue to reveal cellular element or treated with polyclonal antibodies to visualise GABA immunoreactive cells, so that the ^{14}C AMS image can be compared with the cellular element and cells that contain GABA.

One immediate by-product of the radiocarbon AMS imaging is the measurement of the ^{14}C concentration, represented as $^{14}C/^{12}C$, averaged over a scanning area. Samples can be dissected out from large brain sections (30–100 μm thickness) mounted in epoxy resin on microscope glass slides as 2 mm (depth of cortex from pia to white matter) by 200 μm stripes at any distance lateral from the injection site. The size fits well with the typical scanning area of 200 μm by 100 μm. Around the injection site, the average ^{14}C concentration is measured to be 2×10^{-6}. The average ratio decreases as the distance along the cortex to the injection site increases. Within 300 μm distance, the ratio decreases to $\sim 10^{-6}$ and more drastically to $\sim 2 \times 10^{-8}$ when the distance is over 3 mm. This indicates the transportation and the selective uptake of C^{14}-GABA by neurons connected to the injection site.

It is possible and useful to obtain the C^{14} and C^{13} or C^{12} scanning images of the same area simultaneously. This can help relate the scanned area to that of its adjacent histological sections of the same tissue elements by identifying and aligning the landmarks such as tissue/resin margins and the blood vessels. The combination of the ^{13}C (^{12}C) and ^{14}C mappings can be linearly colour coded according to the $^{14}C/^{13}C$ ratio at each pixel, with blue for ^{13}C reading only changing gradually to green, orange and red where maximum ratio of $^{14}C/^{13}C$ is recorded. As there is no detectable C^{14} for pure resin areas, the blood vessels that filled with the pure resin and tissue/resin margins should record only C^{13} and be blue in colour. This feature can be easily identified in the pseudo-colour image. This is further helped by the slightly greater carbon ion yield for pure resin than that for tissue. Because the samples are sectioned serially at 0.5 μm thick, the contours of blood vessels, neurons and tissue/resin margins do not vary much in terms of shape and size for the adjacent sections so they can be used as landmarks. Therefore, these "landmarks" enable the carbon isotope images be accurately matched with the optical microscopic images of the stained adjacent sections. Hence, the activities of cells and their processes can be identified. A typical result is shown in Fig. 2.

Fig. 2. Top: ^{14}C and ^{13}C AMS image of 0.5 μm thick tissue/resin sample. Bottom: Toluidine blue stained adjacent section. In the AMS image, the colour is coded according to $^{14}C/^{13}C$ ratio from blue (low) to red (high). Label c: capillary; white arrows: tissue/resin margin; pink circle and black arrow: ^{14}C labelled neuron; black arrow head: unlabelled neurons. The colour image can be accessed at http://www.rlaha.ox.ac.uk/leaf_bio.html

At the current resolution, we are able to see large ^{14}C "hotspots" (in red and orange) and the blood vessels and resin margins (in blue, marked as c). The features have good repeatability for separate scans with some of the scans taken weeks apart and at different positions. The larger hotspots are about 8 ~ 15 μm in diameter and can be matched with the neurons in histologically toluidine blue stained adjacent sections indicating the selective uptake of GABA. In the figure, the radiocarbon labelled neuron (marked by a pink circle) was also shown in the AMS scan of the subsequent sections. With the blood vessels labelled as c and the margin (pointed to by a white arrow), it matches well with the large neuron in toluidine blue stained section. The low level ^{14}C labelling of the neuropil between cells, which reduces the overall contrast in ^{14}C signal to a factor of about 20, is thought to be

caused by the GABA uptake by different oriented neuronal axons and dendrites as well as synaptic terminals of a size of 0.1 to 1 μm, too small to be resolved. With some other sections (not shown here), it is even possible to relate the C^{14} labelled patch to a myelinated axons of 0.3–0.6 μm. This demonstrates that the uptake of the transmitter occurs at the nerve terminals close to the injection site and is transported retrogradely to the neurons through the neuronal axons. There are also areas with no radiocarbon (indicated by a black arrow head). These correspond to unlabelled neurones either because their axons are not connected to the site of injection or they are simply not GABAergic (GABA uptake mechanism is absent), even though they are surrounded by the terminals or are next to the GABAergic neurons. There are some greenish patches that can also be related to the neurons. This indicates that the GABA uptake is moderate: the neurons may not be as well connected to the injection site as the heavily labelled one (in red and orange). The observations of the distribution of ^{14}C-labelled GABA agrees well with the GABA immunoreactive image. That is, the radiocarbon labelled neurons are GABA reactive neurons, while the unlabelled ones are neurochemically different, lack endogenous GABA is evident from the immunostained sections. As expected, glial cells are labelled as they take up GABA, particularly those close to the injection site where the labelled GABA concentration is the highest.

We have also studied the metabolism of ^{14}C labelled leucine by neurons in the auditory area of baby gerbils. A total radioactivity of between 2 μCi and 10 μCi of leucine of duly concentrated solution are injected into the blood circulation of gerbils after the surgical deafening of one ear. A period ranging from 1 ~ several hours is allowed for the metabolism to take place. The brain tissue in the area is then histologically prepared as previously described, sectioned and AMS scanned. The average ^{14}C concentration has been measured to be 6×10^{-8} indicating the amino acid has been taken up and incorporated into proteins within the developing neurons. It was anticipated that the neurons in the deafened area would die and cease to develop. Further work has been planned to make a quantitative comparison.

4. Conclusions and discussion

We have demonstrated that imaging AMS can be successfully applied to reveal the radiocarbon distribution in biological system at one micron resolution. In combination with histological techniques, even smaller tissue elements can be identified. The performance of the ^{14}C-AMS imaging compares very favourably with autoradiographic methods and with ordinary SIMS as the required labelling concentration is much lower (as much as two orders of magnitude), the ^{14}C ratio measurement is more accurate and the background is much lower. The radioactive dosage we used is between 0.15 μCi to 10 μCi, much lower than that required for autoradiography and SIMS. For a typical scanning area of 200 μm × 100 μm, the image is made up of 100 × 100 pixels with dwell time of 30 ms. The total duration is 5 min. The resolution is currently limited to 1 μm, the spot size of the primary ion beam, but 0.2–0.1 μm is possible as the Ga^+ microprobe of that spot size is commercially available. This may require a higher label concentration from the current 10^{-8} to 5×10^{-6} for 0.1 μm resolution. As the sample preparation by resin embedding and thin sectioning is a common procedure for biologists and histologists, this new technique should be easily applied to other fields. The AMS images can be correlated with those obtained with TEM and so it may be possible to locate receptors and ion channels on the surface of neurons and other cells or cellular elements using suitably selective ^{14}C-labelled ligands. We believe the technique has great potential in studying the metabolism, interactions and chemical communications at inter- and intra-cellular levels in the brain and other biological systems.

Acknowledgements

This work has been carried out with the financial support of the MRC Brain and Behaviour Centre and the MRC Anatomical Neuropharmacology Unit. We are grateful to Dr David Moore and Dr Ann Markham of Physiology Department, Oxford University for preparing gerbil samples, Dr Stewart Freeman of Lawrence Livermore National Laboratory for providing stimulating discussions and Dr Z. Nusser of MRC Anatomical Neuropharmacology Unit for the preparation of test samples at the initial stages of the development.

References

[1] P. Fragne, C. Briancon, C. Fourre, J. Clerc, O. Casiraghi, J. Jeusset, F. Omri and S. Halpern, Biol. Cell 74 (1992) 5.
[2] C. Bronk Ramsey and R. E. M Hedges, Nucl. Instr. and Meth. B 52 (1990) 322.
[3] Z. X. Jiang, C. Bronk Ramsey and R. E. M. Hedges, SIMS X Proc., ed. A Benninghoven (Wiley, London, 1996), in press.
[4] S. P. H. T. Freeman, C. Bronk Ramsey and R. E. M. Hedges, Nucl. Instr. and Meth. B 92 (1994) 231.
[5] D. Elmore, Biol. Trace Element Res. 12 (1987) 231.
[6] D. L. Martin, in: GABA in Nervous System Function, eds. E. Roberts, T. N. Chase and D. B. Tower (Raven Press, New York, 1976) pp. 347–386.
[7] K. C. Y. Sie and E. W. Rubel, J Comp. Neuro. 320 (1992) 501.